Open access • Journal Article • DOI:10.1063/1.462639

Collisional energy transfer in highly excited molecules: Calculations of the dependence on temperature and internal, rotational, and translational energy

David L. Clarke, I. Oref, Robert G. Gilbert, Kieran F. Lim

Published on: 01 Jan 1992 - Journal of Chemical Physics (American Institute of Physics)

Topics: Internal energy, Thermal energy, Excited state and Ground state

Collisional energy transfer in highly excited molecules: Calculations of the dependence on temperature and internal, rotational, and translational energy

David L. Clarke, I. Oref, Robert G. Gilbert, and Kieran F. Lim

Citation: The Journal of Chemical Physics **96**, 5983 (1992); doi: 10.1063/1.462639
View online: http://dx.doi.org/10.1063/1.462639
View Table of Contents: http://scitation.aip.org/content/aip/journal/jcp/96/8?ver=pdfcov
Published by the AIP Publishing

Collisional energy transfer in highly excited molecules: Calculations of the dependence on temperature and internal, rotational, and translational energy

David L. Clarke, I. Oref,[a] and Robert G. Gilbert
School of Chemistry, University of Sydney, Sydney. NSW 2006, Australia

Kieran F. Lim
Department of Chemistry, University of New England, Armidale, NSW 2351, Australia

(Received 16 September 1991; accepted 6 January 1992)

Classical trajectory calculations of the rate of collisional energy transfer between a bath gas and a highly excited polyatomic method, and the average energy transferred per collision, as functions of the bath gas translational energy and temperature, are reported. The method used is that of Lim and Gilbert [J. Phys. Chem. **94**, 72 (1990)], which requires only about 500 trajectories for convergence, and generates extensive data on the collisional energy transfer between Xe and azulene, as a function of temperature, initial relative translational energy (E'_T), and azulene initial internal energy (E'). The observed behavior can be explained qualitatively in terms of the Xe interacting in a chattering collision with a few substrate atoms, with the collision duration being much too brief to permit ergodicity but with a general tendency to transfer energy from hotter to colder modes (both internal and translational). At thermal energies, trajectory and experimental data show that the root-mean-squared energy transfer per collision, $\langle \Delta E^2 \rangle^{1/2}$, is relatively less dependent on E' than the mean energy transfer $\langle \Delta E \rangle$. The calculated temperature dependence is weak: $\langle \Delta E^2 \rangle^{1/2} \propto T^{0.3}$, corresponding to $\langle \Delta E_{\text{down}} \rangle \propto T^{0.23}$. Values for the calculated average rotational energy transferred per collision (data currently only available from trajectories, and required for falloff calculations for radical–radical and ion-molecule reactions) are of the order of $k_B T$, and similar to those for the internal energy; there is extensive collision-induced internal-rotational energy transfer. The biased random walk "model B," as discussed in text, is found to be in accord with much of the trajectory data and with experiment. This suggests that energy transfer is through pseudorandom multiple interactions between the bath gas and a few reactant atoms; the "kick" given by the force at the turning point of each atom–atom encounter governs the amount of energy transferred. Moreover, a highly simplified version of this model explains why average energies transferred per collision for simple bath gases have the order-of-magnitude values seen experimentally, an explanation which has not been provided hitherto.

I. INTRODUCTION

This paper reports the results of trajectory calculations for the transfer of energy by collision between a highly excited substrate molecule (azulene) and a bath gas (xenon). The aim of the calculations is to elucidate the phenomenological nature of this process and to provide tests for approximate models. The long-term objective is to provide means of calculating energy transfer data with sufficient accuracy for predicting or fitting falloff data in unimolecular and recombination reactions[1] (which requires a knowledge of the rate coefficients both for collisional energy transfer and for reaction) and experiments such as the "physical" methods[2] (also denoted "direct" methods) which infer energy transfer data from spectroscopic observations of a nonreacting molecule. The energies of the substrate molecule involved in such situations are about 10^3–10^5 cm^{-1}, and the densities of states of the substrate molecule are extremely high (e.g., 10^{10}–10^{30} states per cm^{-1}).

An efficient basic methodology for carrying out essentially exact classical calculations of the requisite quantities has recently been deduced.[3] Applications of the method to systems where reliable experimental data are available show[4] that acceptable accord between trajectories and experiment is to be expected, given commonly used potential functions, for all except the lightest bath gases. For this reason, we choose a system for the present studies (highly excited azulene colliding with Xe), where the trajectory data and experiments for thermal systems are in good agreement. The poor accord earlier reported[4] between trajectories and experiments for the lightest bath gases, He and Ne, can probably be ascribed to lack of knowledge of the substrate/bath gas interaction potential, rather than to any quantum effects. This is because a series of experiments involving changes of masses of the lightest atoms in both reactant[5] and bath gas,[6,7] wherein any quantum-mechanical effects should re-

[a] Permanent address: Department of Chemistry, Technion–Israel Institute of Technology, Haifa 32000, Israel

 0021-9606/92/085983-16$06.00

sult in large changes in energy transfer rates, showed no such changes and, hence, there is strong *experimental* evidence that a classical description is quite adequate for the purposes at hand.[8] Since quantum effects should be negligible, and since trajectory data give good accord with experiment for the systems studied in the present paper, the trajectories should accurately mimic the true dynamics of the system.

We explore here the dependence of the energy transfer rate on temperature, initial internal energy, final rotational, and internal energy, and substrate/bath gas relative translational energy (this last requires extensions, given in Sec. II, to our original[3] method for obtaining the requisite energy transfer quantities from classical trajectories). These variations were chosen because they provide insight into the dynamics of the energy transfer process, they suggest explanations and make predictions as to the important question of the temperature dependence of the average energy transferred per collision, they provide information on the average *rotational* energy transferred in collisions of highly excited molecules, data which are currently completely unavailable from experiment but which are important in interpreting and predicting falloff curves for processes (such as radical–radical recombinations and ion-molecule reactions) which require this information.[9] Moreover, the data can provide useful insight on approximate models for collisional energy transfer.

In the last context, it is important to compare "exact" theory (accurate trajectory treatment of the dynamics, for a given interaction potential) with approximate theory (the predictions of an approximate, or model, treatment of the dynamics, using the *same* potential function). Such a comparison is much more informative than a comparison of an approximate model with actual experiment, since the model involves approximations in *both* the interaction potential and the dynamics, and no firm conclusions can be drawn if model and experiment disagree (which is wrong, potential, approximate dynamics, or both?) or agree (which may be caused by a fortuitous cancellation of the separate errors in potential and dynamics).

The energy transfer which is the subject of this paper is quantified as $R(E,E')$: The rate coefficient for transfer from initial energy E' to final energy E. The dimensions of R are (energy concentration time)$^{-1}$. It is essential to inquire just what amount of detail is necessary to predict falloff curves and the results of "physical" experiments. Data from such experiments are usually relatively insensitive to the full details of the distribution function $R(E,E')$ (i.e., of its dependence on both E and E'), but rather depend only on the values of one (or, for certain experiments, two) moment(s) of this distribution. We denote the nth moment as $R_{E',n}$,

$$R_{E',n} = \int_0^\infty (E - E')^n R(E,E') dE. \tag{1}$$

$R_{E',1}$ is the mean rate of energy transfer and $R_{E',2}$ is the mean-square rate; a knowledge of either of these quantities (when used in a solution of the master equation) usually suffices, for example, to predict a falloff curve satisfactorily (given the energy dependence of the microscopic reaction rate coefficients). The first moment can be directly inferred from experiment using "physical" methods; the second moment (as will be explained below) is easier to compute (and, as will be amplified later in the text, the two moments can be readily interconverted).

The necessity of only having to calculate a single moment, rather than the full distribution function, renders calculations of energy transfer quantities in such systems achievable with relatively moderate computational resources. Only about 500 trajectories need to be found to obtain a properly converged value of the second moment. Previously, less trajectories were thought necessary;[4] the need for the increase is discussed in Appendix A, wherein is also discussed a new method for estimating the uncertainty in rate parameters deduced using the present technique. The method of Lim and Gilbert[3] (and the extensions deduced in the present paper), together with the availability of a public domain program[10] for executing these trajectories and (most importantly) for properly selecting the initial conditions, has now rendered such calculations relatively routine. It should be pointed out that there have been many classical trajectory studies of such collisional energy-transfer problems;[11–20] however, the only method available for actually obtaining the requisite energy-transfer *rates* in a computationally efficient way appears to be that of the present authors.[3] An equally valid approach to interpreting experimental data is to solve *both* the energy transfer *and* master equation problems simultaneously.[11–13] The computational requirements are approximately the same as those for implementation of the two techniques separately. The simultaneous technique does not readily permit a physical interpretation of the average energy transfer rate coefficients.

Although the experimental observables, and the results of a trajectory calculation, are always some *rate coefficient*, it is common (and very useful for conceptual and model building purposes) to reexpress such rates on a *per collision* basis, through some arbitrary, but physically reasonable (e.g., Lennard-Jones or hard-sphere) collision number Z. For this purpose, one defines the *probability per collision*, $P(E,E')$,

$$P(E,E') = \frac{1}{Z} R(E,E') \tag{2}$$

and the corresponding moments such as the average energy transferred per collision $\langle \Delta E \rangle$ (sometimes denoted $\langle \Delta E_{\text{all}} \rangle$) and the mean-square energy transferred per collision $\langle \Delta E^2 \rangle$ by

$$\langle \Delta E^n \rangle = \frac{1}{Z} R_{E',n}. \tag{3}$$

It is essential[3,21] to emphasize that it is the rates, and not the per collision quantities, which are the observables. Indeed, it is impossible, for all except hard spheres, ever to define a "collision," since the substrate/bath gas interactions are of infinite extent and, hence, it is impossible to calculate quantities such as $\langle \Delta E \rangle$ directly from trajectories. "Per collision" quantities can always be deduced trivially from the corresponding rates once Z has been defined, but such a definition is arbitrary (although should be chosen in a sensible way so as to aid intuition and model building).

II. DERIVATION OF CLASSICAL TRAJECTORY FORMULAS

We wish to study the variation of the energy transfer rates with internal and rotational energy of the substrate, and with the substrate/bath gas relative translational energy. The chosen method[3] for obtaining such rates from trajectories was deduced for a *canonical* (i.e., constant temperature) system. We now derive the methodology by which average energy transfer rate coefficients can be obtained from trajectory calculations for a *microcanonical* system; i.e., one in which the translational energy of the bath gas/substrate is fixed. This is a straightforward extension of the result derived previously.[3]

Consider a substrate molecule colliding with a bath gas with a fixed relative initial translational energy E'_T. We wish to calculate the classical rate coefficient for transfer, by collision, from an initial energy E' to a final energy E. E' and E may refer to (1) the total energy of the molecule E or (2) the energy in the "inactive" external rotational degrees of freedom $E_{\rm rot} = I\omega^2$, where I is the value of the two equal principal moments of inertia of a symmetric top (or the geometric mean $I = \sqrt{I_a I_b}$ of the two nearly equal ones for an asymmetric top) and ω is the corresponding angular speed or (3) the internal energy $\epsilon = E - E_{\rm rot}$, defined as the energy in the "active" degrees of freedom (the vibrational degrees of freedom plus the rotational energy about the third principal axis).[1,22,23]

The classical rate coefficient $M(E,E';E'_T)$ for this microcanonical collisional process is given by[24]

$$M(E,E';E'_T) = \frac{\int d\mathbf{p}\, d\mathbf{q}\,\delta[E - H_{\rm subs}(t\to\infty)]f(\mathbf{p},\mathbf{q})\ (p_1/\mu)\ \delta(q_1 - q_1^0)}{\int d\mathbf{p}\, d\mathbf{q} f(\mathbf{p},\mathbf{q})} \tag{4a}$$

$$= \nu \int_0^\infty 2\pi b\, db \mathbb{P}(E'_T,b;E,E'), \tag{4b}$$

where the integrals are over all of phase space whose positions and momenta are $\mathbf{p}$ and $\mathbf{q}$, q_1 is the bath-gas substrate relative translational coordinate, q_1^0 is a large value of this coordinate where trajectories are started, $p_1/\mu = \nu$ is the corresponding velocity, $E'_T = \frac{1}{2}\mu\nu^2$, $f(\mathbf{p},\mathbf{q})$ is the distribution function describing the appropriate initial conditions, $H_{\rm subs}$ is the Hamiltonian for the substrate molecule, b is the impact parameter, and $\mathbb{P}(E'_T,b;E,E')$ is the classical probability for the process (in this case, transfer by collision of the internal energy from E' to E). For simplicity, we have assumed that the bath gas is structureless. Changing variables from ν to E'_T and noting that, for the purposes of trajectory calculations, the limit of the integration over impact parameter is changed to a sufficiently large but finite value b_m, one has

$$M(E,E';E'_T) = \left(\frac{2E'_T}{\mu}\right)^{1/2} \int_0^\infty 2\pi b\, db \mathbb{P}(E'_T,b;E,E')$$

$$= \lim_{b_m\to\infty} \left(\frac{2E'_T}{\mu}\right)^{1/2} \pi b_m^2 \tag{5a}$$

$$\times \int_0^{b_m} \frac{2\pi b}{\pi b_m^2}\, db \mathbb{P}(E'_T,b;E,E'). \tag{5b}$$

In Eq. (5b) we have deliberately multiplied and divided by πb_m^2, to bring out the dependence on the cross-section-like term. The nth moment $M_{E',n}$ is given by

$$M_{E',n} = \left(\frac{2E'_T}{\mu}\right)^{1/2} \times \int_0^\infty \int_0^\infty dE(E - E')^n 2\pi b\, db \mathbb{P}(E'_T,b;E,E'). \tag{6}$$

At this point we note the relation between the microcanonical rate coefficient $M(E,E';E'_T)$ and the canonical one $R(E,E';T)$,

$$R(E,E';T) = 2\pi^{-1/2}(k_B T)^{-3/2} \times \int_0^\infty dE'_T (E'_T)^{1/2} e^{-E'_T/k_B T} M(E,E';E'_T). \tag{7}$$

For the moments $R_{E',n}$

$$R_{E',n} = \left(\frac{8k_B T}{\pi\mu}\right)^{1/2} \frac{1}{(k_B T)^2} \times \int_0^\infty \int_0^\infty \int_0^\infty db\, 2\pi b\, dE(E - E')^n dE'_T E'_T \times e^{-E'_T/k_B T} \mathbb{P}(E'_T,b;E,E') \tag{8}$$

and so

$$R_{E',n} = 2\pi^{-1/2}(k_B T)^{-3/2} \times \int_0^\infty dE'_T (E'_T)^{1/2} e^{-E'_T/k_B T} M_{E',n}(E'_T). \tag{9}$$

As stated, it is very useful to reexpress such rates on a *per collision* basis, through some arbitrary, but physically reasonable, collision number Z, e.g., that for hard spheres of radius d,

$$Z_{\rm can} = \left(\frac{8k_B T}{\pi\mu}\right)^{1/2} \pi d^2 \quad \text{(canonical)}, \tag{10a}$$

$$Z_{\mu\rm can} = \left(\frac{2E'_T}{\mu}\right)^{1/2} \pi d^2 \quad \text{(microcanonical)}. \tag{10b}$$

The relations between the rate coefficients and the per collision quantities are then

$$M_{E',n} = Z_{\mu\rm can} \langle \Delta E^n \rangle_M, \tag{11}$$

where $\langle \Delta E^n \rangle_M$ is the microcanonical nth moment of the energy transferred per collision. We note for later use that Eqs. (9)–(11) lead to the result

$$\langle \Delta E^n \rangle = \frac{1}{(k_B T)^2} \int_0^\infty dE_T E_T e^{-E'_T/k_B T} \langle \Delta E^n \rangle_M. \quad (12)$$

For notational convenience, we shall henceforth drop the M subscript for the microcanonical quantities $\langle \Delta E^n \rangle_M$, where no ambiguity arises.

We now turn to the means of evaluating Eq. (6) from a finite number of classical trajectories. If these trajectories are chosen from appropriate statistical weightings in all internal variables of the substrate (e.g., random vibrational phases and orientations) following the usual method of orthant and/or microcanonical sampling,[25,26] and the impact parameter is chosen from the distribution $2\pi b/\pi b_m^2$, one then simply has:[3]

$$M_{E',n} = \left(\frac{2E'_T}{\mu}\right)^{1/2} \lim_{b_m \to \infty} \lim_{N \to \infty} \frac{\pi b_m^2}{N} \sum_{i=1}^{N} (\Delta E_i)^n, \quad (13)$$

where ΔE_i is the energy change in the ith trajectory and N is the number of trajectories. Equation (13) is the basic algorithm for finding the required average energy-transfer quantities. Note that the dimensions of $M_{E',n}$ are (volume) (time^{-1}) (energy)^n. The corresponding formula for computation of $\langle \Delta E^n \rangle_M$ is

$$\langle \Delta E^n \rangle_M = \lim_{b_m \to \infty} \lim_{N \to \infty} \left(\frac{b_m}{d}\right)^2 \frac{1}{N} \sum_{i=1}^{N} (\Delta E_i)^n. \quad (14)$$

Convergence in N is generally quickest if one calculates the second moment ($n = 2$), rather than the first moment, since then one is always summing positive quantities. Despite their deceptively simple appearance (which is to take the average of the energy transfer of a large number of trajectories), it is essential to realize that Eqs. (13) and (14) are only valid provided the initial conditions are chosen with the correct sampling.

We now deduce the microscopic reversibility relationship for $M(E,E';E'_T)$. This corresponds to that for the canonical rate coefficient $R(E,E';T)$,

$$f(E')R(E,E';T) = f(E)R(E',E;T), \quad (15)$$

where $f(E) = \rho(E) \exp(-E/k_B T)/Q$, $\rho(E)$ being the density of states of substrate, and $Q = \int \rho(E) \times \exp(-E/k_B T) dE$ the partition function. Equation (15) arises from the time-reversible property of classical (and quantum) mechanics: The flux of trajectories forwards and backwards must be the same. From Eq. (9) it can then be seen that the microcanonical microscopic reversibility relationship is

$$M(E,E';E'_T)\rho(E')(E'_T)^{1/2} = M(E',E;E_T)\rho(E)(E_T)^{1/2}. \quad (16)$$

Recall that the initial total and translational energies are the primed quantities E' and E'_T and the final ones are unprimed. By conservation of energy $E' + E'_T = E + E_T$.

III. METHOD OF APPLICATION TO Xe/AZULENE

For azulene colliding with xenon, earlier trajectory studies[4] had shown that (under circumstances discussed below) agreement with experimental results[27–31] could be obtained using a potential function made up of bends, stretches, torsions, and wags for the azulene, and atom–atom Lennard-Jones 12-6-4 interaction for the Xe/azulene interaction (the r^{-4} interaction being used to mimic the dipole of the azulene[4]). The potential for the present study, which has the same functional form as but differs slightly in numerical values from that given previously,[4] is

stretches: $\frac{1}{2} f_s (r_{ij} - r_{eq})^2$,

bends: $\frac{1}{2} f_\theta (\theta_{ijk} - \theta_{eq})^2$,

out-of-plane wags: $\frac{1}{2} f_\alpha (\alpha_{jkmn} - \pi)^2$,

generalized Lennard-Jones: $\frac{a}{r_{ij}^{12}} + \frac{b}{r_{ij}^{6}} + \frac{c}{r_{ij}^{4}}$,

torsions: $V_0 \sin^2 \tau_{ijklmn}$,

where r_{ij} is the distance between atoms i and j, θ_{ijk} is the angle between atoms i, j, and the central atom k, α_{jkmn} is the angle between the normal to the plane defined by the atoms j, m, and n and the line segment between atoms k and the central atom j, and τ_{ijklmn} is the angle between the two planes IJK (containing il and parallel to jk) and LMN (containing il and parallel to mn). The potential parameters are given in Table I. The numbering system used for the atoms is as follows: The carbon atoms obey the standard IUPAC numbering scheme for azulene,[32] the hydrogen numbering follows directly on such that atom 11 is the hydrogen bonded to the carbon labeled atom 1 and so forth, and the xenon atom is number 19. The frequencies obtained from a normal-mode analysis of the azulene potential so defined are generally within a few cm^{-1} of those of Lim and Gilbert[4] (wherein is given a comparison with experimental frequencies) but reducing, by approximately 20%, the average discrepancy between experimental and theoretical frequencies (note that the earlier paper inadvertantly omitted two of the experimental frequencies which can however be easily obtained from the original source).

The trajectories were calculated using our public domain program MARINER,[10] itself a derivative of the public domain program MERCURY.[33] Initial internal energies were chosen to correspond to those used in experimental studies on this system (about 17×10^3 and 30×10^3 cm^{-1}, as discussed later. Note here that the data of Barker and coworkers are obtained for an average energy somewhat less than these, which are those of the Göttingen group; however, the differences in mean-squared energy-transfer values resulting from these differences are relatively small). Rotational energies were chosen from a thermal distribution at 300 K. Initial conditions were otherwise chosen as prescribed earlier. The maximum impact parameter b_m was varied to ensure adequate convergence; it was found that 9 Å was sufficient for all cases studied. The initial center-of-mass separation was 16 Å. The number of trajectories required to evaluate Eq. (13) to adequate convergence was about 500 in all cases, as explained in Appendix A. The values of transla-

TABLE I. Potential parameters for the azulene/xenon interaction. For brevity obviously symmetry related force constants are not included.

Atom i	Atom j	r_e (Å)	f_s (mdyn Å^{-1})
		Stretches	
1	2	1.404	8.433 50
3	10	1.404	8.100 94
4	10	1.380	8.501 16
4	5	1.391	8.501 16
5	6	1.385	8.332 73
9	10	1.490	6.132 68
1	11–18	1.084	5.000 00

Atom i	Atom j	Atom k	θ_{eq} (deg)	f_θ (mdyn Å rad^{-1})
		Bends		
2	9	1	107.10	0.572
2	11	1	126.45	0.572
1	3	2	111.50	0.572
1	12	2	124.25	0.572
5	10	4	130.10	0.572
5	14	4	114.95	0.572
4	6	5	128.00	0.572
4	15	5	116.00	0.572
5	7	6	130.20	0.572
5	16	6	114.90	0.572
1	8	9	126.00	0.572
1	10	9	107.20	0.572

Atom j	Atom k	Atom m	Atom n	f_α (mdyn Å rad^{-2})
		Out-of-plane wags		
1	11	2	9	0.45[a]

Atom i	Atom j	a kcal mol^{-1} Å^{12}	b kcal mol^{-1} Å^{6}	c kcal mol^{-1} Å^{4}
		Generalized Lennard-Jones		
1	19	$0.344\,40\times10^{7}$	$-0.129\,79\times10^{4}$	$-0.464\,50\times10^{1}$
2	19	$0.344\,40\times10^{7}$	$-0.129\,79\times10^{4}$	$-0.341\,61\times10^{-2}$
4	19	$0.344\,40\times10^{7}$	$-0.129\,79\times10^{4}$	$-0.326\,36\times10^{-1}$
5	19	$0.344\,40\times10^{7}$	$-0.129\,79\times10^{4}$	$-0.303\,96\times10^{-3}$
6	19	$0.344\,40\times10^{7}$	$-0.129\,79\times10^{4}$	$-0.262\,63\times10^{-1}$
9	19	$0.344\,40\times10^{7}$	$-0.129\,79\times10^{4}$	$-0.112\,50\times10^{-2}$
11–18	19	$0.112\,73\times10^{7}$	$-0.555\,21\times10^{3}$	0.0

Atom i	Atom j	Atom k	Atom l	Atom m	Atom n	V_0 kcal mol^{-1}
			Torsions			
1	9	11	2	3	12	7.084 80
3	2	13	10	4	9	6.432 48
10	3	9	4	5	14	6.326 64
4	10	14	5	6	15	7.171 20
5	4	15	6	7	16	6.900 12
9	1	8	10	3	4	4.329 72

[a] Similarly for all analogous out-of-plane wags.

tional energy were chosen to cover the thermal and suprathermal range [0.7–10 kcal mol^{-1}; 1 kcal mol^{-1} = 4.184 kJ mol^{-1}; $2RT \approx 1.2$ kcal mol^{-1} at $T = 300$ K; the factor of 2, not the usual factor of 1.5, relating the mean translational energy and the temperature, arises because of the $E_T \exp(-E_T/k_BT)$ in Eq. (12)]. Values of the initial internal energy E' were chosen as 30 644 and 17 500 cm^{-1}, corresponding to those in the experiments of Barker and of the Göttingen group.[27–31]

IV. RESULTS AND QUALITATIVE OBSERVATIONS

Trajectory calculations produce more numerical results than one is able to deal with in a sensible fashion. For this reason, we present "slices" through a very extensive set of data. For convenience, these are given as "per collision" quantities, with the re-scaling of rates carried out using Eqs. (3) and (10), using a hard-sphere diameter $d = 6.97$ Å (corresponding to the collision number $Z_{can} = 478\times10^{-18}$ m^3 s^{-1} of Hippler *et al.*[31]).

First, we compare, in Table II, our present results with experiments and with our previous study. The "experimental" entries for $\langle\Delta E^2\rangle^{1/2}$ were obtained from the experimental $\langle\Delta E\rangle$ using the biased random-walk model (BRW) for $P(E,E')$ as described later; trajectory $\langle\Delta E\rangle$ entries were also obtained in a similar fashion from the corresponding $\langle\Delta E^2\rangle^{1/2}$. The good agreement of $\langle\Delta E^2\rangle^{1/2}$ trajectory val-

TABLE II. Comparison of energy-transfer values from trajectory simulations and "direct" experiments at 300 K. All values normalized to $Z_{ref} = 478 \times 10^{-18}$ m^3 s^{-1} (Ref. 31).

E' (cm^{-1})	This work	Lim and Gilbert[a]	Göttingen group[b,c]	Barker *et al.*[c,d]
		$-\langle \Delta E \rangle$ (cm^{-1})		
30 644	150 ± 22	116	225	222
	205 ± 20[e]	154[e]		
17 500	105 ± 23	102	160	110
	185 ± 25[e]	133[e]		
		$\langle \Delta E^2 \rangle^{1/2}$ (cm^{-1})		
30 644	430 ± 30	323	420	417
17 500	415 ± 40	306	347	273

[a] Reference 4.
[b] References 30 and 31.
[c] $\langle \Delta E^2 \rangle$ values obtained from $\langle \Delta E \rangle$ using BRW.
[d] References 27–29.
[e] $\langle \Delta E \rangle$ values obtained from $\langle \Delta E^2 \rangle$ using the BRW functional form as explained in text.

ues with experiment has been retained even with the minor changes in the potential-energy surface; most importantly, the present calculations have much improved statistics which, *inter alia*, include now a sufficiently large number of trajectories to take accurate account of supercollisions.[34] The present calculations reproduce (at least semiquantitatively) the experimental dependence of the average energy transfer on initial energy, in addition to reproducing the absolute values. This suggests that the present calculations should adequately model the actual dynamics of the systems studied.

Some microcanonical results are shown in Figs. 1–3, which give the computed mean and mean-square, energy transferred per collision as a function of the translational energy E'_T, for the two different values chosen for E', for the total (E), rotational (E_{rot}), and internal (ϵ) energy transfer; statistical uncertainties in these quantities are also shown (see Appendix A). Note that $\langle \Delta E \rangle = \langle \Delta E_{rot} \rangle + \langle \Delta \epsilon \rangle$, but of course an equivalent additive relationship does not hold for the mean-square quantities.

There are some discernible trends in the data as follows.

At the highest translational energy the net energy transfer is upward and clearly more so for the *lower* E'. On the other hand, at the lowest translational energies $\langle \Delta E \rangle$ for $E' = 3 \times 10^4$ cm^{-1} is more negative than that for $E' = 1.7 \times 10^4$ cm^{-1}; i.e., the net energy transfer is downwards and more so for the *higher* E'—the difference is only slightly greater than the uncertainties. The $\langle \Delta E \rangle$ curves for the two E' values remain very close through to intermediate E'_T.

$\langle \Delta E \rangle$ changes sign at about $E'_T = 2$ kcal mol^{-1}, a change in the net direction of the average energy transfer close to thermal energies. This effect is equivalent to the sign change with change in temperature in canonical systems, which is well understood.[2,35]

$\langle \Delta E_{rot} \rangle$ on the other hand is always positive. As a corollary, $\langle \Delta \epsilon \rangle$ changes sign at an energy above 2 kcal mol^{-1} (recall $\langle \Delta E \rangle = \langle \Delta E_{rot} \rangle + \langle \Delta \epsilon \rangle$).

All total mean-square energy-transfer quantities exhibit a minimum around $E'_T = 1.2$ kcal mol^{-1}; the mean-energy quantities may show small maxima or points of inflexion at about the same E'_T but such effects are of the same order as the statistical uncertainty.

At low E'_T, there is a considerable amount of collision-induced *intramolecular* internal/rotational ($\epsilon \leftrightarrow E_{rot}$) energy transfer. There is relatively little *total* energy transfer but the average rotational and internal energy transfers are both large in magnitude and of opposite sign.

For these systems the changes in internal and rotational

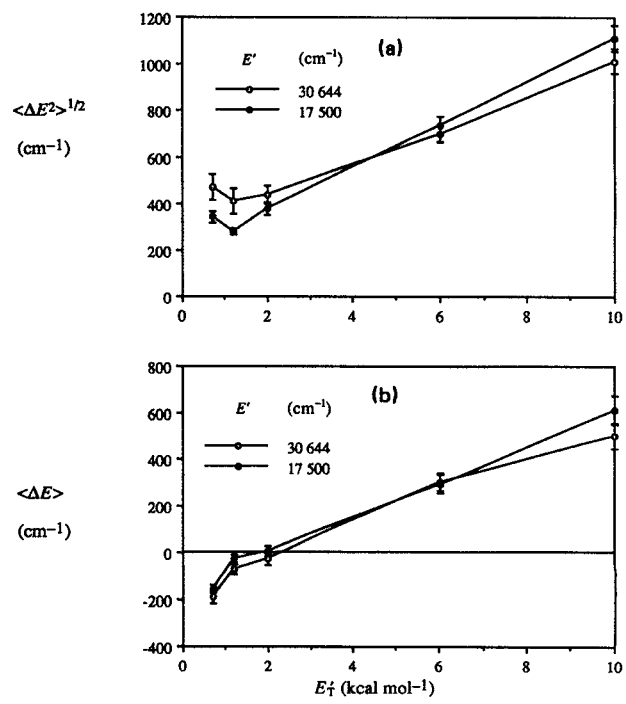

FIG. 1. Variation of (a) root-mean-square and (b) mean, total (internal plus rotational) energy transferred per collision for azulene/Xe collisions as a function of the initial azulene internal energy (17 500 and 30 644 cm^{-1}) and the azulene/Xe relative translational energy. The error bars represent the average deviation as determined by the bootstrapping.

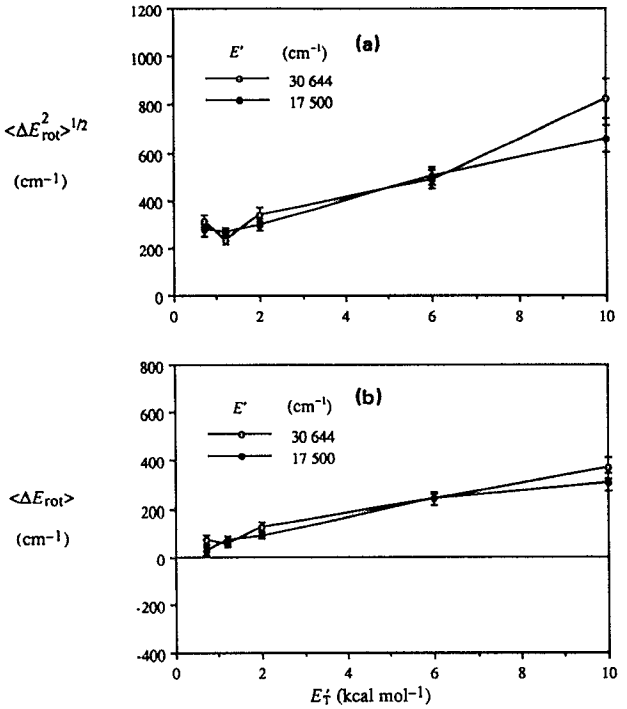

FIG. 2. Variation of (a) root-mean-square and (b) mean, rotational energy transferred per collision for azulene/Xe collisions as a function of the initial azulene internal energy (17 500 and 30 644 cm^{-1}) and the azulene/Xe relative translational energy. The error bars represent the average deviation as determined by the bootstrapping.

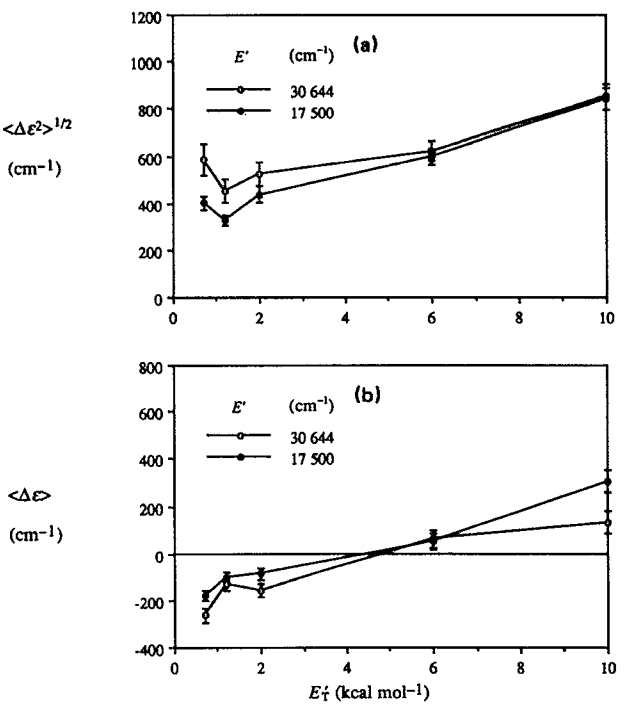

FIG. 3. Variation of (a) root-mean-square and (b) mean, internal energy transferred per collision, for azulene/Xe collisions as a function of the initial azulene internal energy (17 500 and 30 644 cm^{-1}) and the azulene/Xe relative translational energy. The error bars represent the average deviation as determined by the bootstrapping.

energy are of similar magnitude: 100–800 cm^{-1} depending on E'_T. The values of $\langle \Delta E^2_{rot} \rangle$ are close to, but somewhat less than, those of $\langle \Delta \epsilon^2 \rangle$ for a given E'_T. These trends can be explained as follows.

Examination of trajectories shows[8,18,34,36,37] that a typical collision is one in which the substrate internal energy exhibits a number of oscillations caused by the interactions of the bath gas with one or more of the substrate atoms. While the collision duration is much too short to allow complete energy randomization between the collision partners (in this case, between the center-of-mass translational degree of freedom and the azulene internal motions), there is a general tendency to transfer energy from hotter to colder modes (both internal and translational). Now, although the initial total energy of the azulene is very high (3×10^4 $cm^{-1} \approx 90$ kcal mol^{-1}), the average energy in a given azulene vibration and, hence, the average energy in the atom interacting with the bath gas at a given moment, will be much less than this. Thus, at very high translational energies, energy will tend to flow from the relatively hotter translation degree of freedom to the colder vibrational degrees of freedom. Furthermore, since the average energy in an azulene atom will be less at an internal energy of 1.7×10^4 cm^{-1} than for 3×10^4 cm^{-1}, more energy will tend to be transferred from the translation at the lower E'. This leads to the values of $\langle \Delta E \rangle$ and $\langle \Delta E^2 \rangle^{1/2}$ being greater for $E' = 1.7\times10^4$ cm^{-1} for the highest E'_T.

For low translational energy, the converse will occur: Energy will be transferred to the now colder translational degree of freedom from the hotter vibrations. Thus, for lower E'_T, $\langle \Delta E \rangle$ will be negative; moreover, since more energy will be transferred from the higher internal energy, $\langle \Delta E \rangle$ for higher E' will be more negative than that for lower E' and, consequently, $\langle \Delta E^2 \rangle^{1/2}$ is greater for the higher E'.

To locate the position of the change in sign of $\langle \Delta E \rangle$, we need to consider some sort of average vibrational energy per mode for azulene. There are a number of ways of defining such a quantity. In the simplest sense this can be taken as the total internal energy divided by the number of modes, giving a value of 2.8 and 3.6 kcal mol^{-1} for $E' = 1.7\times10^4$ and 3×10^4 cm^{-1}, respectively (remembering that for a classical simulation, the total energy available for transfer includes the zero-point energy). A more sophisticated means of expressing an average energy per mode is as follows.[38] One first defines a vibrational temperature T_v in terms of the total vibrational partition function Q_v using $E'_{tot} = RT_v^2(\partial \ln Q_v/\partial T_v)$, where E'_{tot} is the sum of E' and the thermal internal energy. Next, $\langle E_v \rangle$ the average energy in a particular mode with vibrational partition function $q_v(T_v)$, can be obtained using the expression $\langle E_v \rangle = RT_v^2(\partial \ln q_v/\partial T_v)$. Since (as discussed later) the highest frequencies are especially involved in the collisional energy transfer process, it has been suggested[38] that this measure of the average energy per mode is better for interpreting energy transfer experiments than the simpler definition given previously. However, for the present purpose of interpreting classical trajectory data (as distinct from actual experiment), one must use classical partition functions; the

average energy per mode then becomes the same with both methods. Moreover, the existence of extensive internal-to-rotational energy redistribution during the collision (see the following) renders improved treatments of the average energy per mode unnecessary for the purpose of qualitative discussion. What is important is that the average energy associated with a mode lies within the translational energy range covered in these studies. The transition between (on average) up and down collisions is therefore placed within this range, which is broad enough to display both the high and low translational energy limits. This explains qualitatively the occurrence and location of the zero in the E'_T dependence of $\langle \Delta E \rangle$. To relate this transition point more accurately to the internal energy of the azulene it would be necessary to have a more complete understanding of the classical dynamics of the distribution of energy within the modes and the rate of intramolecular vibrational redistribution, a point which is not pursued further here. Moreover, the statistical uncertainty in the calculated energy transfer values makes it difficult to address the relative order in $\langle \Delta E \rangle$ for the two internal energies for intermediate translational energies, since the calculated values are quite close in this range. Indeed, a classical simulation may not be expected to accurately model such small differences in energy transfer between two internal energies, because of the neglect of zero-point-energy effects.

The average rotational energy transfer always being positive can be seen as a result of the effective rotational temperature being much lower than the vibrational and (for higher E'_T) translational temperatures. That is, there is always another mode (internal or translational) with an energy greater than that initially in the rotational modes, which therefore always increase in energy after a collision.

The origin of the small maxima and points of inflection at about 1 kcal mol^{-1} is unclear. It may arise partly because the initial rotational energy was chosen from a thermal distribution at 300 K ($k_B T \approx 0.6$ kcal mol^{-1}), but the complex dynamical interactions between rotational, translational, and vibrational degrees of freedom preclude a clear-cut explanation from the limited trajectory data currently available.

In an isolated molecule, the total angular momentum is conserved and, hence (to a good approximation), $E_{\rm rot}$ is constant; the passage of the bath gas breaks down this conservation temporarily and, hence, collision-induced rotational-internal energy transfer can take place. The actual amount of this exchange depends on the amount of rotational-internal coupling induced by the presence of the bath gas, this coupling being different from the internal-translational and rotational-translational coupling that is the cause of bath-gas/substrate total energy transfer. In light of the discussion earlier, we suggest that the amount of collision-induced rotational-internal energy transfer can be qualitatively understood in terms of the difference between the rotational and internal temperatures. If this difference is much greater than those between translational temperature and the internal and rotational temperatures, then there will be more collision-induced rotational-internal energy transfer than translational-total energy transfer. Since the rotational-internal temperature difference is independent of the translational temperature, collision-induced rotational-internal energy transfer, therefore, is most apparent at lower E'_T where there is no dominating internal-translation temperature difference. However, a complete understanding of this effect must await quantitative explanation of the division of the energy transfer into internal and rotational components.

The actual magnitude of the energy transferred will be explained when we consider an approximate quantitative model for the dynamics in Sec. V and in Appendix B. It is noteworthy that, while experimental values for changes in internal energy are of course now known for many systems, no such data are available (except for very small molecules) for *rotational* energy transfer of highly excited species. Concerning the relative values of $\langle \Delta E^2_{\rm rot} \rangle$ and $\langle \Delta \epsilon^2 \rangle$ (or alternatively of $\langle \Delta E_{\rm rot} \rangle$ and $\langle \Delta \epsilon \rangle$), we have no further qualitative or quantitative explanation for the observed partitioning into rotational and internal components and can note that the trajectory data given here should prove useful for future investigations of this question.

Having discussed the behavior of the microcanonical results, we examine how the average energy transfer depends on E' in the canonical case, for which trajectory data at 300 K are shown in Table II. The sensitivity to E' of $\langle \Delta E \rangle$ and $\langle \Delta E^2 \rangle^{1/2}$ may be quantified as the relative variation $(d\langle \Delta E \rangle/dE')/\langle \Delta E \rangle$, which is about 1×10^{-5} per cm^{-1}; the corresponding quantity for $\langle \Delta E^2 \rangle^{1/2}$ is about 0.5×10^{-5} per cm^{-1}. Hence (at 300 K), $\langle \Delta E \rangle$ is twice as sensitive to E' as is $\langle \Delta E^2 \rangle^{1/2}$. That is, at thermal energies, the mean-square energy transfer values show a relatively smaller variation with initial energy E' than do those of $\langle \Delta E \rangle$. Note, however, that at suprathermal energies, the E' dependencies of both $\langle \Delta E \rangle$ and $\langle \Delta E^2 \rangle^{1/2}$ are about the same.

The experimental variation of $\langle \Delta E \rangle$ with E' at thermal energies has been the subject of considerable debate in the literature.[27–31] Now, the interconversion between $\langle \Delta E \rangle$ and $\langle \Delta E^2 \rangle$, obtained from Eqs. (1) and (3) given a functional form for $P(E,E')$, is quite insensitive to the form of $P(E,E')$. This is exemplified in Fig. 4, which shows $\langle \Delta E \rangle$ as a function of $\langle \Delta E^2 \rangle^{1/2}$ for azulene at 300 K with three different functional forms for $P(E,E')$: exponential down,[1] biased ran-

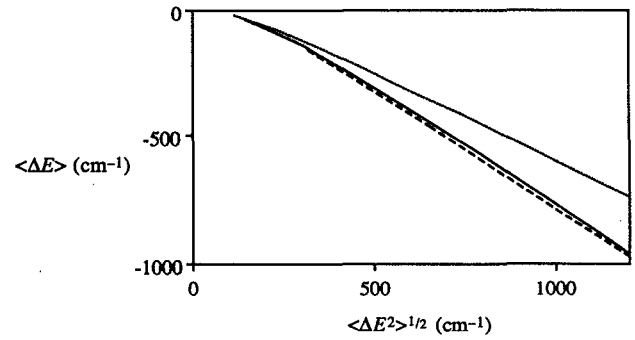

FIG. 4. Value of mean-energy transferred per collision as a function of the root-mean-square value for azulene with $E' = 17\,500$ cm^{-1} for $T = 300$ K, for biased random-walk (—), $(E-E')^2 \exp[(E-E')/\alpha]$-down (···), and exponential-down (---) models for $P(E,E')$.

dom walk[1] [which has a displaced Gaussian functional form; see Appendix B], and a model with $P(E,E') \propto (E-E')^2 \exp[-(E'-E)/\alpha]$ for $E<E'$. These three models have qualitatively different functional forms. In generating the results of Fig. 4, the integral expressions for $\langle \Delta E \rangle$ and $\langle \Delta E^2 \rangle$, Eqs. (1) and (3), were evaluated numerically with the functional form for $P(E,E')$ only being used to generate the downward ($E'>E$) values, the upward values being found exactly using microscopic reversibility. This exact numerical integration avoids having to make assumptions such as an exponential form for the equilibrium population distribution required to generate these quantities using approximate analytic formulas;[1] i.e., microscopic reversibility is taken into account exactly in Fig. 4. The requisite methodology for this[1] is available as public code.[39] Note that although the illustration given here of the insensitivity to the functional form is for a canonical system, it must also hold for a microcanonical one, since $M(E,E';E'_T)(E'_T)^{1/2}$ and $R(E,E';T)$ are related by a Laplace transform, as shown in Eq. (7). One sees from Fig. 4 that the relationship between $\langle \Delta E \rangle$ and $\langle \Delta E^2 \rangle^{1/2}$ is indeed insensitive to the functional form for $P(E,E')$, except for very large energy transfer ($>1000\ \mathrm{cm}^{-1}$). Further calculations (not illustrated here) show that this insensitivity is even better at higher temperatures.

The relative sensitivities to E' of $\langle \Delta E \rangle$ and $\langle \Delta E^2 \rangle$ can now be examined with reference to experiment, using the data of Barker and co-workers.[27–29] These experiments measure $\langle \Delta E \rangle$ (or rather infer the values of $R_{E',1}$ after calibration), but the values of $\langle \Delta E \rangle$ can be converted with minimal uncertainty to equivalent values of $\langle \Delta E^2 \rangle^{1/2}$ through Fig. 4. Figure 5 shows, for the monatomic bath gases, the experimental ratios of the mean energy transfer and root-mean-square energy transfer, for experiments where the initial excitation is about 17 500 and 30 644 cm^{-1}. If the $\langle \Delta E^2 \rangle^{1/2}$ values were exactly independent of initial energy, the ratio for this quantity should be unity; the data show an average value of 1.4. On the other hand, the corresponding average ratio for $\langle \Delta E \rangle$ is 1.9. This indeed suggests that, for thermal

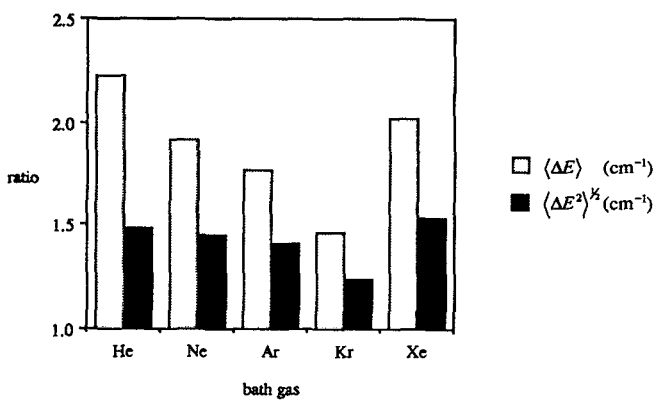

FIG. 5. Ratio of average energy transferred per collision at two different initial excitation energies $\langle \Delta E \rangle (30\,644\ \mathrm{cm}^{-1})/\langle \Delta E \rangle (17\,500\ \mathrm{cm}^{-1})$ and corresponding ratio for mean-squared energy transfer $\langle \Delta E^2 \rangle (30\,644\ \mathrm{cm}^{-1})/\langle \Delta E^2 \rangle (17\,500\ \mathrm{cm}^{-1})$. Experimental $\langle \Delta E \rangle$ values are from Barker (Refs. 27–29).

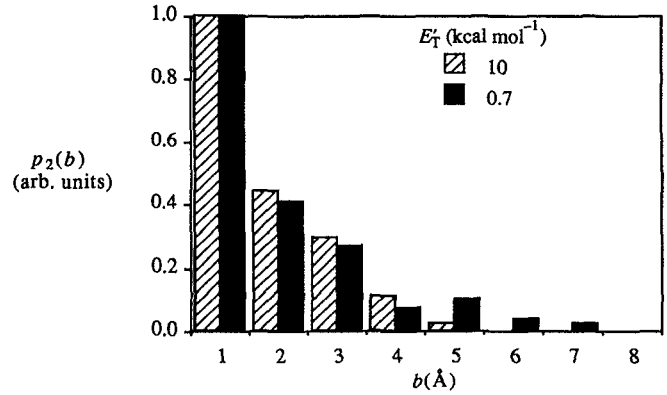

FIG. 6. Pseudo-opacity functions $p_2(b)$ for subthermal microcanonical ($E'_T = 0.7$ kcal mol^{-1}) and suprathermal ($E'_T = 10$ kcal mol^{-1}) azulene/Xe collisions; $E' = 1.7\times10^4\ \mathrm{cm}^{-1}$.

systems, $\langle \Delta E^2 \rangle^{1/2}$ is less sensitive to E' than is $\langle \Delta E \rangle$. This observation will be of use in Sec. V when we are considering quantitative models for the energy-transfer process. The trajectory data also show that the mean *rotational* energy-transfer quantities $\langle \Delta E_{\mathrm{rot}} \rangle$ and $\langle \Delta E^2_{\mathrm{rot}} \rangle$ are also only weakly dependent on the initial total energy E'. This is illustrated in Fig. 2.

Finally, we note the behavior of the *opacity function* $p_n(b)$ for collisional energy transfer. This quantity is defined in the usual way except that it has different units from conventional opacity functions (as appropriate to the units of the dynamical quantity we are considering); e.g., we define the microcanonical opacity function by rewriting Eq. (6) as

$$M_{E',n} = \int_0^\infty 2\pi b\, db\, p_n(b). \tag{17}$$

The $p_n(b)$ are easily obtained from trajectory data. Typical opacity functions for high and low translational energy are shown in Fig. 6 [note that owing to the small number of trajectories chosen by the sampling procedure for small b, large $p_n(b)$ values at small b may possibly be artifactual]. The opacity function for $E'_T = 0.7$ kcal mol^{-1}, which is slightly lower than thermal energies, shows that even though the maximum is at small b, there are significant contributions out to large impact parameters where many energy-transferring collisions are such that the bath gas interacts in a chattering collision with atoms on the periphery of the substrate molecule. The opacity function for a *suprathermal* system (10 kcal mol^{-1}) shows slightly different behavior. Now there is only a significant contribution to the energy transfer from small impact parameters. This can be understood when it is noted that high E'_T implies a high centrifugal angular momentum barrier for a given b; thus trajectories at higher b will tend to be deflected by this barrier at higher translational energies and, hence, never approach sufficiently closely to exchange much energy.

Next, we consider the implications that the translational energy dependence of Fig. 1 has for the temperature dependence of the average energy-transfer quantities. First, we note that a more detailed inspection of the translational energy dependence of Fig. 1 shows that the dependence at lower

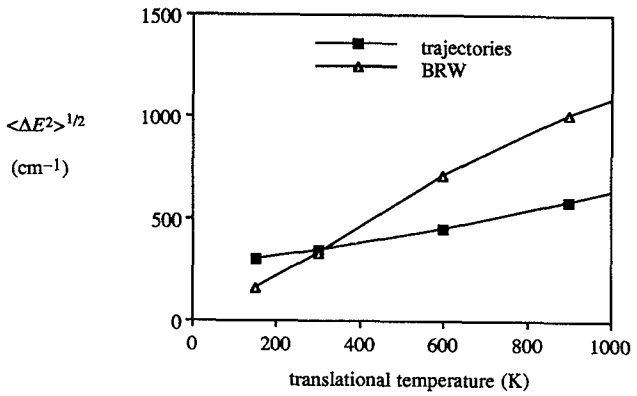

FIG. 7. Comparison of values for root-mean-square total energy transfer from trajectories and from biased random-walk model B, for azulene/Xe with $E' = 17\,500\ \mathrm{cm}^{-1}$.

energies is different from that at higher energies due to the net change in the direction of energy transfer around thermal energies; as stated, this is likely to arise because the initial rotational energy was chosen from a thermal distribution in the present simulations. The calculated *temperature dependence* of the root-mean-square energy transfer is depicted in Fig. 7, obtained from our predicted translational energy dependence by using the data of Fig. 1 for direct numerical integration of Eq. (12). The data of Fig. 7 can be approximated by $\langle \Delta E^2 \rangle \propto T^{0.3}$ over the ambient thermal energy range of 250–600 K: a weak but positive temperature dependence. This can be compared with the temperature-dependent energy-transfer data for $\langle \Delta E_{\mathrm{down}} \rangle$ for N_2 bath gas.[40] It was found that $\langle \Delta E_{\mathrm{down}} \rangle \propto T^{-1/2}$, which when converted to values of the mean-square energy transfer, yields $\langle \Delta E^2 \rangle^{1/2} \propto T^{-0.43}$. While our calculated exponent for monatomic bath gas is opposite to the observations for diatomic bath gas, what is important is that both experiment and theory show a very weak temperature dependence. It must be borne in mind that both experimental and predicted dependencies are very weak and, as is apparent from Fig. 2, the translational energy (and hence temperature) dependence is strongly influenced by the average rotational energy transferred per collision. Hence, the calculated temperature dependence for Xe bath gas is probably significantly influenced by our choice of initial rotational energy from a thermal distribution at 300 K. Moreover, it is likely that the observed experimental temperature dependence with N_2 bath gas has a large contribution from transfer of rotational energy of the N_2.

Note that if the translational energy dependence of $\langle \Delta E^2 \rangle_M$ can be approximated by

$$\langle \Delta E^2 \rangle_M = \sum_{i=0}^{\infty} a_i (E'_T)^i, \tag{18}$$

then Eqs. (18) and (12) give

$$\langle \Delta E^2 \rangle = \sum_{i=0}^{\infty} \Gamma(i+1) a_i (k_B T)^i. \tag{19}$$

This has the implication that if the E'_T dependence of $\langle \Delta E^2 \rangle_M$ could be approximated as a single exponent i, so also can the temperature dependence of $\langle \Delta E^2 \rangle$.

V. QUANTITATIVE COMPARISON OF TRAJECTORY DATA WITH BIASED RANDOM-WALK MODEL

In Sec. IV we showed how much of the trajectory data could be understood qualitatively in terms of the dynamics of the energy-transfer event. In this section we shall use the trajectory data obtained here, as well as trajectory data reported elsewhere, to make a *quantitative* comparison with the assumptions and predictions of a particular model. We reiterate that a definitive test of the dynamical assumptions inherent in an approximate model can only be properly carried out by comparing accurate trajectory treatment of the dynamics, for a given interaction potential, with the predictions of a model, using the *same* potential function. Such a comparison is more informative than that between an approximate model with actual experiment since the model involves approximations in *both* the interaction potential and the dynamics, and no conclusions as to the correctness of either the model or the assumed potential can be drawn whether or not model and experiment disagree or agree.

There are a number of models for the collisional energy-transfer process in the literature[2] and we do not propose to review these here. Rather, our aim is to see if any of the general observations from the trajectory data can support the assumptions of a particular model and then to carry out quantitative tests against the trajectory results. It will emerge that what has been denoted "model B" of the biased random-walk treatment[41] is in accord with trajectory results.

Our starting point is the observation, from Sec. IV, that the mean-square energy transfer is less dependent upon the initial energy than is $\langle \Delta E \rangle$. One of the models in the literature, the BRW model B,[41] has among its assumptions the supposition that $\langle \Delta E^2 \rangle$ is *independent* of E'; given the relatively weak dependence evinced by both the trajectory calculations and experiment, it is not unreasonable to take an E' independent $\langle \Delta E^2 \rangle$ as an approximation which is in qualitative accord with these data. The model (presented in detail elsewhere[36,37,41,42]) is summarized for convenience in Appendix B. It takes note of the results of trajectory calculations that show that the substrate internal energy during a collision exhibits a large number of pseudorandom oscillations. These oscillations arise from the "chattering" nature of the energy-transfer interaction: Multiple collisions of the bath gas with one or more single substrate atoms driven by the highest-frequency oscillations, which have random phase. Given the assumption of randomness, subject to the constraint of microscopic reversibility, a functional form for $P(E,E')$ can then be obtained using the theory of Brownian motion: The displaced Gaussian of Eq. (B2) of Appendix B. This functional form contains a single parameter s, which is obtained [Eq. (B4) of Appendix B] from the product of the collision duration (t_c) and a diffusion coefficient in "energy space" (D). The BRW model then makes dynamical approximations to obtain a simple expression for D, for a given interaction potential. The oscillations are treated in an average way with a particular average energy and subject to an

average (atom–atom) force. The crucial approximation in the present context of model B is stated in Eq. (B6) of Appendix B: That this, average oscillator energy (which appears in several different places in the approximate dynamical treatment) is simply the average substrate/bath gas translational energy, independent of the internal energy of the substrate. The alternative version of the BRW model denoted as "model *A*,"[41] incidentally, assumed instead a form for this average energy which depends strongly on E'; this hypothesis can now be rejected because of the availability of the new trajectory data which form the subject of this paper.

A most important result from the BRW model B treatment is that, in its most primitive version, it leads to an expression, Eq. (B18) of Appendix B, which explains in a very simple fashion the typical values of the energy transferred per collision observed experimentally with monatomic bath gases which no other model currently available is able to do.

Since the BRW model B makes a hypothesis which is in accord with a prominent feature of the present trajectory data, it is profitable to use the current data to test this model quantitatively. It is important to note that the BRW model B contains *no semiempirical parameters*, in contrast to some alternative versions.[36,41]

Before starting such a comparison it is realized that there is a difficulty in comparing the results of *microcanonical* (constant translational energy) trajectory data with the predictions of any approximate *canonical* (constant temperature) model, as is the BRW model. Of course, one could attempt to derive a microcanonical version of the model, but that is a nontrivial exercise. This is because of the relationship between the up and down energy-transfer rates imposed by microscopic reversibility. These microscopic reversibility relations are imposed by the time reversibility of quantum and classical mechanics, and any approximate model which does not obey them is seriously flawed. In the BRW model,[36,37,41,42] canonical microscopic reversibility is imposed on the dynamical assumptions from the outset. However, the microscopic reversibility relations for the microcanonical and canonical cases, Eqs. (15) and (16), are inherently different in nature. For the canonical case, the temperature is the same before and after a collision and so does not need to be treated explicitly. In Eq. (15) one has $f(E,T)$ and $f(E',T)$ and the problem is a two-variable one in E and E', with only a parametric dependence on T. For the microcanonical case, however, the translational energy is different before and after the collision, and this must be taken into account specifically, making the problem a three-dimensional one in E, E', and E'_T. Moreover, this additional dimensionality means that the numerical methods used (for example) for solving the master equation and interconverting different averages of $R(E,E')$,[1] which take microscopic reversibility exactly into account *canonically*, can no longer be used in the *microcanonical* case.

This difficulty can be overcome by numerically integrating the $\langle \Delta E^2 \rangle_M$ as a function of E'_T to yield, from Eq. (12), $\langle \Delta E^2 \rangle$ as a function of T, which can then be used for comparison of model and trajectory data of the canonical results

TABLE III. Lennard-Jones parameters used in biased random-walk calculations. For a full description of the origin of these parameters see Ref. 1.

	ϵ (K)	σ (Å)
Azulene/Xe	347	5.33
Xe/Xe	230	4.05
C/C	20.3	3.2
H/H	6.5	3.0

and predictions, given in Fig. 7 (here the trajectory data are for $E' = 17\,500\ \text{cm}^{-1}$). The "local" atom–atom potential functions used in the BRW calculations were taken to be the appropriate averages of those used in the trajectory calculations (parameters are given in Table III). It will be recalled that $\langle \Delta E^2 \rangle^{1/2}$ is found from the trajectory data to be only weakly dependent on E', and also that the BRW model B gives a $\langle \Delta E^2 \rangle^{1/2}$ that is only very weakly dependent on E'; this is seen in Eqs. (B2) and (B18) of Appendix B. It is apparent that although the temperature dependence computed from the trajectory data is not well reproduced by the model, there is reasonable accord between model and trajectory results at lower temperatures. Overall, considering the uncertainties involved, the accord is encouraging seeing that (as stated) the BRW model B contains no semiempirical parameters.

Further tests are now discussed. For this, we return to trajectory data for canonical systems. Figure 8 shows recalculated energy-transfer results (using 600 trajectories rather than 150, which had previously been published[4]), wherein the bath gas was varied. It can be seen again that the accord between trajectory data and BRW model B predictions is very good for the heavier bath gases, but that the dynamical approximations in the BRW model B result in a great underestimate of the energy transfer for the lightest bath gases (He and Ne). This underestimate probably arises because the lightest bath gases are more likely to bounce off the substrate after the first (few) atom–atom encounters and, hence, re-

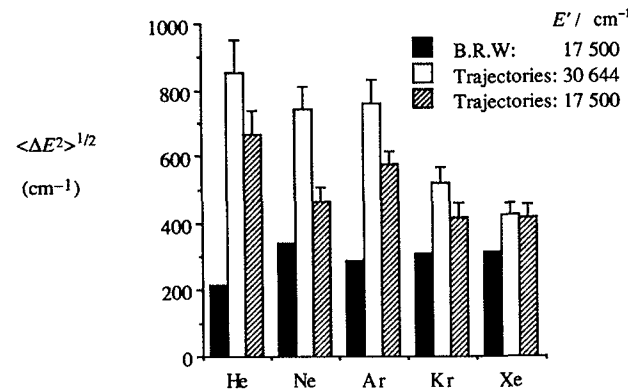

FIG. 8. Comparison of $\langle \Delta E^2 \rangle^{1/2}$ values predicted by BRW model B and obtained from trajectory results for different bath gases at $E' = 1.7 \times 10^4\ \text{cm}^{-1}$ for a canonical system with $T = 300$ K. The error bars represent the average deviation as determined by the bootstrapping.

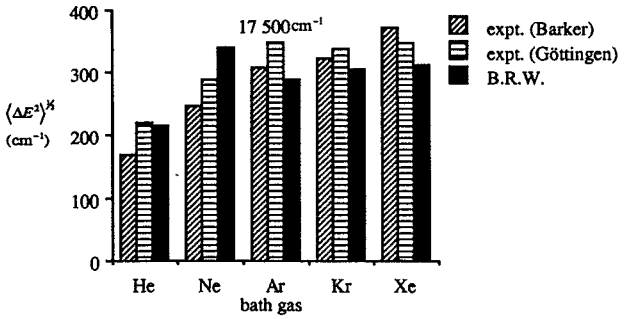

FIG. 9. Comparison of $\langle \Delta E^2 \rangle^{1/2}$ values from BRW model B with values deduced from experimental values of $\langle \Delta E \rangle$ [those of Barker and coworkers (Refs. 27–29) and of the Göttingen group (Refs. 30 and 31)] using method described in text.

duce the chattering nature of the collision which forms the cornerstone of the BRW model.

While the underestimate of the amount of energy transfer for the lightest bath gases by the BRW model B is a cause for concern, it is in the opposite direction to the overestimate of the energy transfer when the trajectory results are compared to experiment.[4] The overestimate of the trajectory calculations is ascribed to the substrate/bath gas interaction potential being too repulsive. It is apparent, for example, from Eq. (B18) of Appendix B, that the average energy transfer is extremely sensitive to the repulsive wall. The quantity F in that equation is the slope of the average atom–atom potential at the classical turning point. Because the underestimate of the approximate dynamics of the BRW model B is opposite to the overestimate caused by the approximate potential, there is a cancellation of errors when the model is compared to experiment, as done in Fig. 9. It is apparent that the approximate model is in good accord with experiment. Experimental trends for the dependence on bath gas are well reproduced by the model. It is however emphasized that this accord for the lightest bath gases is due to a cancellation of errors, and such accord cannot be relied upon to hold in all cases for light bath gases. The model predicts that $\langle \Delta E^2 \rangle^{1/2}$ is essentially independent of E' and thus gives qualitative and semiquantitative accord with the experimental trend of $\langle \Delta E \rangle$ with E'.

VI. CONCLUSIONS

The present paper reports the results of trajectory calculations designed to explore the dependence of rates of collisional energy transfer of highly excited molecules on temperature, translational, rotational, and internal (largely vibrational) energy. These calculations have been carried out for a system where such trajectory calculations have been shown to give good accord with experiment and should therefore properly mimic the real dynamics. The observed behavior can be explained qualitatively in terms of the Xe interacting in a chattering collision with a few substrate atoms, with the collision duration being much too brief to permit ergodicity but with a general tendency to transfer energy from hotter to colder modes (both internal and translational). The results of this paper can be looked upon as predictions of experiments that could, in principle, be carried out; however, their main value is in leading to understanding of the dynamics of this complex process.

One conclusion reached from the present calculations is that the average rotational energies transferred per collision (data currently only available from trajectories, and required for falloff calculations for radical–radical and ion-molecule reactions) are of the order of $k_B T$, and similar to those for the internal energy. The temperature dependencies of the mean-square and average downward energy transferred per collision are small and dependent on the rotational component(s). Another conclusion to be reached from these trajectory data is that the root-mean-square energy transferred per collision is 50% less sensitive to the initial internal energy than is the mean energy transferred; this conclusion is also borne out by deducing values for $\langle \Delta E^2 \rangle^{1/2}$ from experimental values for $\langle \Delta E \rangle$.

The relative insensitivity of $\langle \Delta E^2 \rangle^{1/2}$ to E' observed in the trajectories lends support to an assumption made in a model for the collision dynamics: the biased random-walk model B. This model gives good quantitative accord with the results of trajectory calculations for all except the lightest bath gases. This is a particularly stringent test, as the same potential parameters were used in both the trajectory results and the approximate model. Fortunately, the poor accord of the model with trajectories for the lightest bath gases results in a compensating error to that induced by the incorrect potential function in the trajectory calculations, so the approximate model, with its approximate potential, gives good accord with experiment, at least in the limited examples considered here. However, such coincidences cannot be always relied upon. Nevertheless, it would appear not unreasonable to use this model to supply good first estimates of average energy transfer parameters for the purposes of fitting and predicting falloff data. Energy-transfer parameters from this model are quick and simple to compute, and indeed the requisite code is part of the current version of our UNIMOL program suite.[39]

Most importantly, the BRW model B gives considerable insight into the nature of the energy-transfer event. This is governed by pseudorandom multiple interactions (a chattering collision) between the bath gas atom and one (or a few) of the reactant atoms, and it is the "kick" given by the force at the classical turning point of each atom–atom encounter that governs the amount of energy transferred; Eq. (B18) of Appendix B gives a simplified formula. Moreover, this primitive version of the model, Eq. (B18) of Appendix B, readily explains why average energies transferred per collision for simple bath gases have the observed order-of-magnitude values seen experimentally, an explanation which has not been provided hitherto.

There are of course many questions raised by these trajectory studies which are left unanswered. Primary among these is the form of the potential function between a substrate and the lightest bath gases (He and Ne); accurate quantum-chemical calculations seem the only way around this problem. Another unanswered question is the way the average energy transfer is partitioned between internal and rotational energy. The answer to this problem is especially

important in fitting and predicting falloff data for ion-molecule reactions (and other systems where the moment of inertia of the transition state considerably exceeds that of reactant). A third problem is how to overcome the errors in the approximations to the dynamics in the BRW model B for the lightest bath gases.

The trajectory methods deduced and employed in this paper (which are in the public domain[10]) and the approximate model which they support, when allied with improved potential-energy surfaces, should become increasingly useful tools for the experimentalist to help understand the dynamics of these energy-transfer processes.

ACKNOWLEDGMENTS

The support of the Australian Research Grants Scheme, of the US–Israel Binational Science Foundation, the German–Israeli Fund for the Promotion of Research, and the Technion Fund for the Promotion of Research, are gratefully acknowledged. Helpful suggestions from Professor Sally Chapman, and from Dr. H. Schranz with regard to error estimation are much appreciated.

APPENDIX A: CONVERGENCE AND ERROR ANALYSIS OF TRAJECTORY CALCULATIONS

In our first calculations[3] using the trajectory method employed here, it appeared that 100–150 trajectories were sufficient for adequate convergence in the mean-square energy transfer. In the calculations reported here, the number of trajectories was considerably extended, and it was found that the apparent convergence reported earlier was artifactual. This was manifested by carrying out several sets of 150 trajectories, using different initial random number seeds. The resulting values of the root-mean-square energy transfer were significantly ($>25\%$) different, whereas each batch of 150 trajectories appeared to converge to much better than this criterion. Another manifestation of this problem was seen when the microcanonical values ($\langle \Delta E^2 \rangle_M^{1/2}$), for different values of E'_T, were employed using Eq. (19) to estimate the canonical one ($\langle \Delta E^2 \rangle^{1/2}$); a discrepancy of 50% was sometimes seen when each of these quantities was calculated using only 150 trajectories (note, however, that this discrepancy was not seen in each case; some such calculations appeared to show good agreement and, hence, such a convergence test must be used over a range of, say, E' values).

It is particularly apparent from the total $\langle \Delta E \rangle$, that the poor convergence is caused by a comparatively small number of trajectories which show a very large energy transfer. The effect of such supercollisions has been seen experimentally,[43–47] and has also been reported in other trajectory data.[48] We have also deduced the explanation for their appearance.[34] Here, however, our concern is their effect on convergence. These supercollisions, although rare, contribute significantly to the final $\langle \Delta E^2 \rangle^{1/2}$, as evaluated from a large number (1000) of trajectories. That these rare supercollisions are indeed the cause of the lack of convergence is apparent when one carries out the convergence tests stated earlier, omitting all trajectories where $\langle \Delta E^2 \rangle^{1/2}$ exceeds, say, about 3 times the average value. One then always obtains satisfactory convergence in only 150 trajectories; however, this convergence is a value that is significantly less than that obtained from a much larger number of trajectories without artificial omission of the rare supercollisions.

Earlier calculations[3] showed an apparent convergence because supercollisions are rare: Only one or two might be found in 150 trajectories. Furthermore, unless these occurred late in the batch, the jump in plots of $\langle \Delta E^2 \rangle$ against N, the number of trajectories, which indicates their presence would not be regarded as significant.

Clearly then, an improved procedure for obtaining true convergence must be found together with some estimate of the uncertainties involved, without resorting to running enormous numbers of trajectories. We suggest that the following scheme will satisfy these requirements.

Firstly, it is evident that a larger number of trajectories needed to be run and for each of these a value of $\langle \Delta E \rangle$ was calculated. We have found that 600 trajectories is appropriate. Next, a large number (1000) of alternative sets of 600 trajectories (or more strictly ΔE_i values) are then created by random selection, *with replacement*, from the original set. That is, it is possible for a particular trajectory to appear more than once in a set. This process is an implementation of a *bootstrap* resampling.[49] The required values of $\langle \Delta E^2 \rangle$ were then calculated out for the individual bootstrap sets using the appropriate version of Eq. (14) and also by examining the intercept of a linear least-squares fit to a plot of $\langle \Delta E^2 \rangle$ against $1/N$ for $N > 200$: A simple extrapolation to an infinite number of trajectories. These values of $\langle \Delta E^2 \rangle$ were then averaged over all bootstrap sets to give the final results. The two different versions of the calculation $\langle \Delta E^2 \rangle$ for the individual sets gave essentially identical results.

This method has the added advantage in that it allows an evaluation of the uncertainty in the trajectories in terms of the average deviation (the average of the absolute value of the deviation from the average) or the standard deviation of the bootstrap sets. The average deviation is the basis for the error bars in the figures. The bootstrap method is based on the assumption that the the original trajectories are a good approximation of the full distribution so that the generated data sets are also good representations. The differences between data sets can therefore provide some indication of the uncertainty in the original set.

APPENDIX B: BIASED RANDOM-WALK B MODEL

We present here a summary of the biased random-walk model B, which was found in this paper to give a good approximation, for all except the lightest bath gases, to the results of the present trajectory calculations. Detailed derivations can be found in earlier work.[36,37,41,42]

The biased random-walk (BRW) model is in two parts. The first gives a general description of the probability distribution $P(E,E')$; this distribution function is characterized by a single parameter s. The second part gives a prescription for the value of s.

1. Functional form of $P(E,E')$

The essence of the BRW model is to assume that energy exchange between the molecule and the bath gas during the

collision is random, subject only to the constraint of microscopic reversibility (and, in a more sophisticated version[37] required for considerations of rotational energy transfer,[9,50] to the constraint of conservation of energy). The distribution function $B(E_i,E',t)$ for the probability of the molecule, with initial internal energy E', having internal energy E_i at time t during the collision, is then given by the Smoluchowski equation for diffusion in some external field,

$$\frac{\partial B}{\partial t} = D\frac{\partial(zB + \partial B/\partial E_i)}{\partial E_i}, \tag{B1}$$

where D is an "energy-space diffusion coefficient" and z is a quantity arising from microscopic reversibility. The probability distribution $P(E,E')$ can then be identified as $B(E_i \equiv E,E',t = t_c)$, where t_c is the duration of a collision. It is of course recognized that there is no rigorous way of defining the beginning and end of a collision, but this assumption of some sharp beginning and end is inherent in developing our approximate model.

If D and z are assumed independent of t and of E_i (a restriction which can be lifted in certain cases discussed elsewhere[42]), then the solution of Eq. (B1) is

$$P(E,E') = (4\pi s^2)^{-1/2}\exp\left(\frac{-(zs^2 + E - E')^2}{4s^2}\right), \tag{B2}$$

where the value of z is identified from the microscopic reversibility relation for $P(E,E')$, the analog of Eq. (15), yielding

$$z = -\frac{\partial \ln f(E)}{\partial E} \tag{B3}$$

and the quantity s, which has the dimensions of energy, is given by

$$s^2 = Dt_c. \tag{B4}$$

Having determined the general functional form for $P(E,E')$, it now remains to determine the parameter s by making further assumptions as to the dynamics of the system.

2. The value of the parameter *s*

There are two quantities to be specified to yield a value of s: t_c and D. The former is taken to be the average time for traversing the spherically averaged substrate-molecule/bath-gas interaction potential $V_{av}(r)$, starting from a closest interaction distance d,

$$t_c = (2\mu)^{1/2}\int_d^{r_0} dr\left[E_{av} - V - E_{av}\left(\frac{b_{av}}{r}\right)^2\right]^{-1/2}. \tag{B5}$$

Here μ is the substrate molecule/bath gas reduced mass ($\mu^{-1} = m_{subs}^{-1} + m_{bg}^{-1}$, where the terms on the right-hand side are the molecular weights of substrate molecule and bath gas, respectively). The average energy in model B is taken as the average substrate molecule/bath gas translational energy,

$$E_{av} = 2k_BT \tag{B6}$$

[recall that this is $2k_BT$ rather than the usual $1.5k_BT$, because of the additional $(E'_T)^{1/2}$ term in Eq. (7)], $b_{av} = \frac{2}{3}d$ is an average impact parameter and r_0 is the classical turning point [i.e., where the quantity in parentheses in Eq. (B5) is zero]. Equation (B6) is crucial in the context of comparison with the trajectory calculations, since it supposes that one of the most important quantities in the model is *independent of the initial energy* (E').

The next step is to specify D. The assumption of randomness yields the result, well known from Brownian motion, that the diffusion coefficient can be obtained from the time integral of the autocorrelation function of the time derivative of the energy during the collision

$$D = \int_0^{t_c}\langle\dot{E}_i(\tau)\dot{E}_i(0)\rangle d\tau. \tag{B7}$$

Again using the theory of Brownian motion, the time evolution of E_i during a collision is assumed to be given by a generalized Langevin equation,

$$\frac{d^2E_i}{dt^2} = -a - \int_{-\infty}^{t} K(\tau)\dot{E}_i(t-\tau)d\tau + X(t), \tag{B8}$$

where a is a quantity related to z, $X(t)$ is a randomly fluctuating "force", and $K(t)$ a memory kernel. The next supposition is that $K(t)$ is exponential,

$$K(t) = (A^2 + C^2)e^{-2At}. \tag{B9}$$

The solution of Eq. (B8) then yields

$$\langle\dot{E}_i(\tau)\dot{E}_i(0)\rangle = \langle\dot{E}_i^2\rangle e^{-At}[\cos(Ct) + (A/C)\sin(Ct)] \tag{B10}$$

[note that the functional form given by Eq. (B10) is in accord with direct evaluations[37,41] of the autocorrelation function from trajectory data] and, hence,

$$s^2 = \langle\dot{E}_i^2\rangle t_c\frac{2A}{A^2 + C^2}. \tag{B11}$$

The quantities then to be determined are $\langle\dot{E}_i^2\rangle$, t_c, A, and C. C (which determines the rate of oscillations in the autocorrelation function) is taken to be given from the highest vibrational frequency, ν_h, of the substrate molecule (this is usually a C–H stretch),

$$C = 2\pi\nu_h. \tag{B12}$$

A, which gives the decay time of the autocorrelation function, is approximated as that due to a constant average force F acting on an average or "local" atom–atom oscillator whose energy is $E_{av} = 2k_BT$,

$$A = F\left(\frac{2}{m_bE_{av}}\right)^{1/2}, \tag{B13}$$

where the average mass m_b is the reduced mass for a substrate atom, $\overline{m} = m_{subs}/n_{atoms}$ (where the substrate molecule contains n_{atoms} atoms), and the difference between m_{subs} and $\overline{m}$ is

$$\frac{1}{m_b} = \frac{1}{m_{subs} - \overline{m}} + \frac{1}{\overline{m}}. \tag{B14}$$

[Eq. (B14) corrects an error in Eq. 34(b) of Ref. 41.] The average force F is approximated by noting that it is the changes at the classical turning point of each local atom–atom interaction that contribute most to the energy transfer, and thus hypothesizing that F is the absolute value of the force due to a local atom–atom potential at the turning point,

$$F = \left| \frac{dV_{\rm loc}^{\rm eff}(r)}{dr} \right|_{r=r_0}, \tag{B15}$$

where $V_{\rm loc}^{\rm eff}(r) = V_{\rm loc}(r) + E_{\rm av}(b_{\rm loc}/r)^2$. Here the average "local" impact parameter is assumed to be given by $b_{\rm loc} = \frac{2}{3}\sigma_{\rm loc}(\Omega_{2,2}^*)^{1/2}$, where $\Omega_{2,2}^*$ is the usual reduced collision integral and (assuming for simplicity that the interaction is Lennard-Jones) $\sigma_{\rm loc}$ is the "local" Lennard-Jones radius $\sigma_{\rm loc}$, i.e., $V_{\rm loc}(r) = 4\epsilon_{\rm loc}[(\sigma_{\rm loc}/r)^{12} - (\sigma_{\rm loc}/r)^6]$. The parameters $\sigma_{\rm loc}$ and $\epsilon_{\rm loc}$ are taken as the averages of those of the substrate atoms (see Table III or Gilbert and Smith[1] for examples).

The mean-square rate of internal energy change, $\langle \dot{E}_i^2 \rangle$, is estimated as the product of the frequency ν_h and some average energy. This average energy is in turn approximated as the average kinetic energy $E_{\rm av}$ minus an average energy change per oscillation period ΔV with the restriction that ΔV not be less than $\frac{1}{2}E_{\rm av}$. This gives

$$\langle \dot{E}_i^2 \rangle = \{\nu_h [E_{\rm av} - \min(|\Delta V|, \tfrac{1}{2}E_{\rm av})]\}^2, \tag{B16}$$

where ΔV is found as follows. Let $\Delta x = (2E_{\rm av}/k)^{1/2}$ be the distance moved by the oscillator, where k is an appropriate force constant. The diminution ΔV can be approximated as $\Delta x dV_{\rm loc}/dx$, evaluated at an average atom–atom distance x. The force constant can be approximated as $k = 4\pi^2 m_{\rm light}\nu_h^2$, where $m_{\rm light}$ is the mass of the lightest atom (it is the lightest atoms that are responsible for the rapid oscillations). The average atom–atom distance x can be approximated as the mean of an outer value ($x/\sigma_{\rm loc} = \frac{7}{6}$, again assuming a Lennard-Jones local interaction and using the average impact parameter as earlier) and an inner one ($x/\sigma_{\rm loc} = 1$). Thus the average x is given by $x/\sigma_{\rm loc} = \frac{5}{6}$. One thus has

$$\Delta V = -34.0 \frac{\epsilon_{\rm loc}}{\sigma_{\rm loc}\nu_h} \left(\frac{E_{\rm av}}{m_{\rm light}} \right)^2. \tag{B17}$$

Equations (B11)–(B17), (B5), and (B6) furnish the complete expressions required to evaluate the parameter s (and hence other energy transfer parameters such as $\langle \Delta E \rangle$ and $\langle \Delta E^2 \rangle^{1/2}$). However, these expressions are hardly physically transparent. It is useful to consider some approximations, which typically might introduce errors of 50%, but which lead to much simpler expressions. First, in Eq. (B11), one notes that usually $A^2 \ll C^2$, and so the former term may be ignored in the denominator. Next, ignoring the terms involving ΔV in Eq. (B17) yields simply

$$s^2 \approx \frac{2t_c F}{\pi^2 \sqrt{m_b}} (k_B T)^{3/2}. \tag{B18}$$

This simplified and approximate expression does indeed lead to physical insight. It states that the energy transfer is dominated by the force at the turning point of a local atom–atom repulsion. Order-of-magnitude substitution (using typical values $t_c \approx 10^{-12}$ s, $F \approx (5\text{–}10) \times 10^{-11} N$, the latter derived from a Lennard-Jones potential using $E_{\rm av} = 2k_B T$, etc.) immediately gives a value of s of about 10^2 cm^{-1} at $T = 300$ K. Since the values of $\langle \Delta E \rangle$ and $\langle \Delta E^2 \rangle^{1/2}$ are the same order of magnitude as s, this back-of-envelope estimate immediately explains the typical size of the energy transferred per collision observed experimentally with monatomic bath gases. This is something no other approximate model is able to do. Moreover, as discussed in Sec. IV, the model [in the more sophisticated version given by Eqs. (B11)–(B17), (B5), and (B6)] successfully reproduces experimental results quantitatively and, even more important, qualitatively (i.e., dependence on bath gas and internal energy).

Equation (B18) is very useful for showing why energy transfer values have the observed order of magnitude, and in developing intuitive understanding of the energy-transfer process. However, it should be noted that more subtle effects such as trends with bath gas and E' are only properly reproduced by Eqs. (B11)–(B17), (B5), and (B6) (Sec. V), which are not as transparent in interpretation as Eq. (B18). Moreover, the functional dependencies on mass and temperature in Eq. (B18) are not as simple as at first sight; F depends implicitly on the potential, on $k_B T$ and on m_b.

[1] R. G. Gilbert and S. C. Smith, *Theory of Unimolecular and Recombination Reactions* (Blackwell Scientific, Cambridge, Mass., 1990).
[2] I. Oref and D. C. Tardy, Chem. Rev. **90**, 1407 (1990).
[3] K. F. Lim and R. G. Gilbert, J. Phys. Chem. **94**, 72 (1990).
[4] K. F. Lim and R. G. Gilbert, J. Phys. Chem. **94**, 77 (1990).
[5] T. C. Brown, K. D. King, and R. G. Gilbert, Int. J. Chem. Kinet. **20**, 549 (1988).
[6] R. G. Gilbert and R. N. Zare, Chem. Phys. Lett. **167**, 407 (1990).
[7] B. M. Toselli and J. R. Barker, Chem. Phys. Lett. **174**, 304 (1990).
[8] R. G. Gilbert, Int. Rev. Phys. Chem. **10**, 319 (1991).
[9] S. C. Smith and R. G. Gilbert, Int. J. Chem. Kinet. **20**, 307 (1988).
[10] W. L. Hase and K. F. Lim, Program package MARINER (a general Monte Carlo classical trajectory computer program). Available from K. F. Lim, Department of Chemistry, University of New England, NSW 2351, Australia.
[11] M. Bruehl and G. C. Schatz, J. Chem. Phys. **89**, 770 (1988).
[12] M. Bruehl and G. C. Schatz, J. Phys. Chem. **92**, 7223 (1988).
[13] G. Lendvay and G. C. Schatz, J. Phys. Chem. **95**, 8748 (1991).
[14] A. J. Stace and J. N. Murrell, J. Chem. Phys. **68**, 3028 (1978).
[15] A. J. Stace, Mol. Phys. **36**, 1241 (1978).
[16] H. Hippler, H. W. Schranz, and J. Troe, J. Phys. Chem. **90**, 6158 (1986).
[17] W. L. Hase, N. Date, L. B. Bhuiyan, and D. G. Buckowkowski, J. Phys. Chem. **89**, 2502 (1985).
[18] N. Date, W. L. Hase, and R. G. Gilbert, J. Phys. Chem. **88**, 5135 (1984).
[19] X. Hu and W. L. Hase, J. Phys. Chem. **92**, 4040 (1988).
[20] A. A. Levitsky, L. S. Polak, and S. Y. Umanskii, Chem. Phys. **88**, 365 (1984).
[21] A. R. Whyte, K. F. Lim, R. G. Gilbert, and W. L. Hase, Chem. Phys. Lett. **152**, 377 (1988).
[22] W. Forst, *Theory of Unimolecular Reactions* (Academic, New York, 1973).
[23] A. R. Whyte and R. G. Gilbert, Aust. J. Chem. **42**, 1227 (1989).
[24] R. N. Porter and L. M. Raff, in *Dynamics of Molecular Collisions*, edited by W. H. Miller (Plenum, New York, 1976), Vol. B, p. 1.
[25] D. L. Bunker, J. Chem. Phys. **37**, 393 (1962).
[26] D. L. Bunker and W. L. Hase, J. Chem. Phys. **59**, 4621 (1973).
[27] J. R. Barker, J. Phys. Chem. **88**, 11 (1984).
[28] J. Shi and J. R. Barker, J. Chem. Phys. **88**, 6219 (1988).
[29] M. L. Yerram, J. D. Brenner, K. D. King, and J. R. Barker, J. Phys. Chem. **94**, 6341 (1990).
[30] H. Hippler, B. Otto, and J. Troe, Ber. Bunsenges. Phys. Chem. **93**, 428 (1989).
[31] H. Hippler, L. Lindemann, and J. Troe, J. Chem. Phys. **83**, 3906 (1985).
[32] R. C. Weast and M. J. Astle, Eds., C.R.C. Handbook of Chemistry and Physics (CRC, Boca Raton, 1986).
[33] W. L. Hase, Quantum Chem. Program Exchange Bull. **3**, 14 (1983).
[34] D. L. Clarke, K. C. Thompson, and R. G. Gilbert, Chem. Phys. Lett. **182**, 357 (1991).
[35] D. C. Tardy and B. S. Rabinovitch, J. Phys. Chem. **89**, 2442 (1985).
[36] R. G. Gilbert, J. Chem. Phys. **80**, 5501 (1984).
[37] K. F. Lim and R. G. Gilbert, J. Chem. Phys. **84**, 6129 (1986).

[38] I. Oref and R. G. Gilbert, paper presented at 24th Jerusalem Symposium: Mode-Selective Chemistry, Jerusalem (1991).
[39] R. G. Gilbert, S. C. Smith, and M. J. T. Jordan, UNIMOL program suite (calculation of fall-off curves for unimolecular and recombination reactions) 1991; available directly from the authors: School of Chemistry, Sydney University, NSW 2006, Australia.
[40] J. R. Barker and R. E. Golden, J. Phys. Chem. **88**, 1012 (1984).
[41] K. F. Lim and R. G. Gilbert, J. Chem. Phys. **92**, 1819 (1990).
[42] R. G. Gilbert and I. Oref, J. Phys. Chem. **95**, 5007 (1991).
[43] H. L. Löhmannsröben and K. Luther, Chem. Phys. Lett. **144**, 473 (1988).
[44] K. Luther and K. Reihs, Ber. Bunsenges. Phys. Chem. **92**, 442 (1988).
[45] A. Pashutzki and I. Oref, J. Phys. Chem. **92**, 178 (1988).
[46] I. M. Morgulis, S. S. Sapers, C. Steel, and I. Oref, Chem. Phys. **90**, 923 (1989).
[47] S. Hassoon, I. Oref, and C. Steel, J. Chem. Phys. **89**, 1743 (1988).
[48] L. Lendvay and G. C. Schatz, J. Phys. Chem. **94**, 8864 (1990).
[49] B. Efron, SIAM (Soc. Ind. Appl. Math.) Rev. **21**, 460 (1979).
[50] S. C. Smith, M. J. McEwan, and R. G. Gilbert, J. Chem. Phys. **90**, 1630 (1989).